International Specialty Conference on Cold-Formed Steel Structures
Wei-Wen Yu International Specialty Conference on Cold-Formed Steel Structures 2018

Nov 7th, 12:00 AM - Nov 8th, 12:00 AM

Web Crippling Behavior of Cold-Formed Ferritic Stainless Steel Unlipped Channels under Interior-One-Flange And End-One-Flange Loadings

Amir M. Yousefi

James B. P. Lim

G. Charles Clifton

Wei-Wen Yu International Specialty Conference on Cold-Formed Steel Structures
St. Louis, Missouri, U.S.A., November 7 & 8, 2018

Web Crippling Behaviour of Cold-Formed Ferritic Stainless Steel Unlipped Channels Under Interior-One-Flange and End-One-Flange Loadings

Amir M. Yousefi[1a], James B.P. Lim*[1], G Charles Clifton[1b]

[a] PhD scholar, Email: amirmohammad.yousefi@aucklanduni.ac.nz

*Associate Professor, E-mail: james.lim@auckland.ac.nz

[b] Associate Professor, E-mail: c.clifton@auckland.ac.nz

Abstract

The web crippling strength of cold-formed ferritic stainless steel unlipped channels subject to interior-one-flange and end-one-flange loading is considered in this paper. A total of 144 results are presented, comprising 36 laboratory and 108 numerical results. These results cover the cases of both flanges restrained and unrestrained to the load and reaction plates. Unlike other work in the literature, the numerical analysis in this paper uses nonlinear quasi-static finite element analysis with an implicit integration scheme, which has advantages over static and quasi-static with an explicit integration scheme analyses, particularly for post buckling predictions of unlipped channels subject to web crippling. The laboratory and numerical investigations show current stainless steel design guidance to be too conservative. In terms of design standards, while no cold-formed stainless steel standard distinguishes between flanges restrained and unrestrained to the load and reaction plates, with each standard providing only one equation to cover both restrained and unrestrained, the web crippling strengths for the flanges unrestrained case were found to be higher than those predicted from SEI/ASCE-8 by as much as 24%. Also, the web crippling strengths for the flanges restrained case are shown to be higher than those predicted from equations found in the literature by as much as 48%. New web crippling design equations are proposed; the proposed equations are shown to be reliable when compared against laboratory and numerical results.

Keywords: Ferritic stainless steel; Unlipped cold-formed steel channels; Finite element analysis; Web crippling strength.

1 Introduction

The use of cold-formed stainless steel channels has become increasingly popular due to its favourable material characteristics, corrosion and heat resistance, recyclability and aesthetic appeal (Li and Young 2017a; Lawson et al. 2015). Amongst all stainless steel material grades, ferritic stainless steel is considered to be the most economically competitive (Cashell and Baddoo 2014). Thin-gauged channel-sections, however, have a risk of localised failure in the web (see Fig. 1), particularly under transverse concentrated loads in the vicinity of the applied load. This paper considers the web crippling strength of unlipped cold-formed ferritic stainless

[1]Department of Civil and Environmental Engineering, The University of Auckland, New Zealand

steel channels subject to interior-one-flange (IOF) and end-one-flange (EOF) loading, with flanges restrained and unrestrained to the load and reaction plates.

Design guidance against web crippling for such cold-formed stainless steel channel-sections are found in SEI/ASCE-8 (ASCE 2002), AS/NZS 4673 (AS/NZS 2001) and EN 1993-1-4 (CEN 2006) (which refers to EN 1993-1-3 (CEN 2006) for carbon steel). However, no cold-formed stainless steel standard distinguishes between flanges restrained and unrestrained to the load and reaction plates i.e. the design guidance only provides a single equation to cover both flange conditions. While AISI S100 (AISI 2016) does provide two equations, these equations were developed for cold-formed carbon steel channels. In the literature, no laboratory tests have been reported for unlipped cold-formed stainless steel channels subject to IOF or EOF loading with either flanges restrained or unrestrained to the load and reaction plates. For stainless steel lipped channels, only Korvink and van den Berg (1994) and Korvink et al. (1995) have tested lipped cold-formed stainless steel channels subject to one-flange loading, but only for the case where the flanges are restrained to the load and reaction plates. From these test results (Korvink and van den Berg (1994) and Korvink et al. (1995)) and also the results by Zhou and Young (2006) on tubular sections under two-flange loading, Zhou and Young (2006) proposed design equations for lipped stainless channels subject to one and two-flange loading. Unlipped channels, however, were not tested and not considered.

Other work in the literature by Li and Young (2017a,b) and Zhou and Young (2013; 2007a,b) also considered the web crippling strength of cold-formed stainless steel tubular sections, but again not for unlipped channels. A study by Lawson et al. (2015) (see Fig. 1b) focussed on the shear and bending behaviour of stainless steel channels lipped channels, and not on the web crippling strength under transverse load. Zhou and Young (2010) and Zhou et al. (2009) carried out test programmes as well as numerical simulation studies on the web crippling strength of aluminium hollow square sections. The Authors have also recently conducted numerical studies on lipped cold-formed stainless steel channels having circular web perforations (Yousefi et al. 2017a,b,c, 2016a,b).Uunlipped channels only under two-flange loadings have also been tested by Yousefi et al. 2017d,e,f). In regards to cold-formed carbon steel, Lian et al. (2017; 2016) and Uzzaman et al. (2012; 2013) have tested lipped channels subject to one and two-flange loading. Gunalan and Mahendran (2015), who used the results for a Direct Strength Method approach in regard to the web crippling strength of lipped channels.

In this research, the web crippling strength of unlipped cold-formed ferritic grade G430 stainless steel channels subject to interior-one-flange (IOF) and end-one-flange (EOF) loading is considered, as shown in Figs. 2 and 3. A total of 144 results are presented, comprising 36 laboratory and 108 numerical results; the cases of both flanges restrained and unrestrained to the load and reaction plates are covered. The finite element analysis (FEA) models developed use quasi-static analyses with an implicit integration scheme in ABAQUS. In most of the previous studies in the literature, static analyses were used. However, as found by Natario et al. (2014a,b), there is not always good agreement in terms of post-buckling behaviour. For this reason, Natario et al. (2014a,b) proposed a quasi-static analyses with an explicit integration scheme. However, as per the ABAQUS manual (2014), an explicit integration scheme requires a large number of time increments, which this leads to a longer computational time. Also, explicit analysis is more appropriate for very large problems, solving high speed discontinuous short-term events, and problems involving stress wave propagation.

The quasi-static FE model is used to carry out a parametric investigation to determine the web crippling strength of unlipped channels having different section sizes, load and reaction plates lengths and thicknesses, as well as to examine the suitability of existing design guidance presented in SEI/ASCE-8 (ASCE 2002), AS/NZS 4673 (AS/NZS 2001) and EN 1993-1-4 (CEN 2006) as well as the equations proposed by Zhou and Young (2006). Using laboratory and finite element results, new web crippling design equations are proposed which are shown to be reliable when compared against laboratory and numerical results.

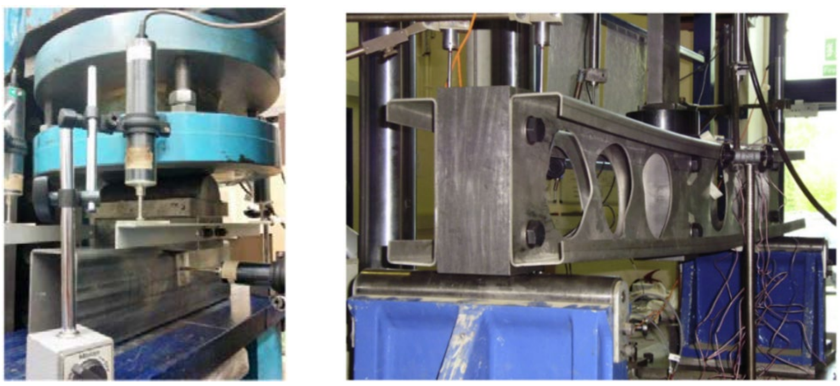

(a) (b)

Fig. 1 Cold-formed stainless steel bearing members; (a) Tubular section after Li and Young (2017a); (b) Lipped channel-section after Lawson et al. (2015)

2 Laboratory study

2.1 Test sections

The ferritic stainless steel unlipped channels were of grade G430 and were press-braked. In total, the results of 36 laboratory tests are considered. The unlipped channels had three different depths that ranged from 175 mm to 250 mm with web slenderness ratio (h/t) ranging between 115.45 and 174.55. The channels length (L) were as per recommendations in AISI S100 Specification (AISI 2016) where the length is three times height of the sections, plus the length of the load bearing plate and two load transfer blocks. The cross-section dimensions measured in the lab as well as notations for determining the parameters are shown in Tables 1 and 2 and Fig. 2. As can be seen in Fig. 3, the load was applied at the centre of the unlipped channels. As shown in Fig. 4, the channels were bolted to the load transfer blocks using 6 mm washer plates.

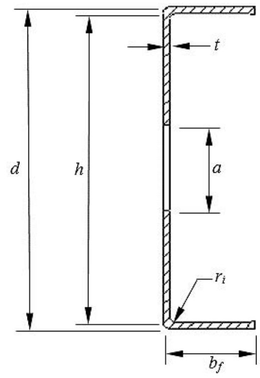

Fig. 2 Definition of symbols

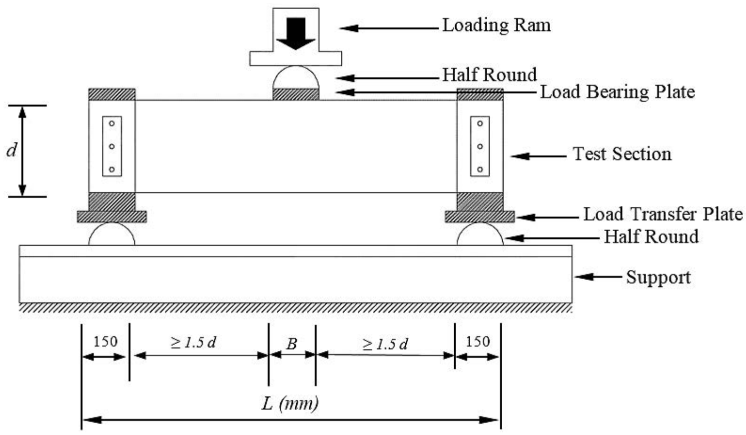

(a) IOF load

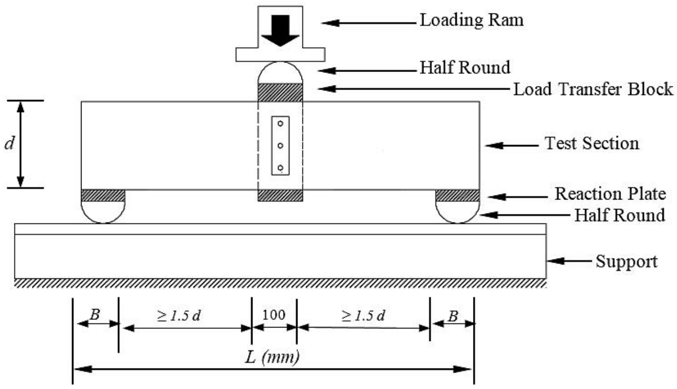

(b) EOF load

Fig. 3 Front view of test arrangement

Table 1 Measured section details and laboratory and finite element ultimate web crippling strengths under IOF load case for both flanges restrained and unrestrained to load bearing plate

Section	Load bearing length	Web depth	Flange width	Web thickness	Filet ratio	Length of channel	Laboratory load full pair	Laboratory load per web	Finite element load per web	Comparison
	B	d	b_f	t	r_i/t	L	P_{LAB}	P_{LAB}	P_{FEA}	P_{LAB}/P_{FEA}
	(mm)	*(mm)*	*(mm)*	*(mm)*	*(mm)*	*(mm)*	*(kN)*	*(kN)*	*(kN)*	
Flange unrestrained										
175x60-t1.5-B50	50	176.09	59.74	1.50	1.00	775.00	20.32	10.16	10.20	1.00
175x60-t1.5-B75	75	176.30	59.69	1.50	1.00	800.00	22.64	11.32	11.19	1.01
175x60-t1.5-B100	100	176.15	59.81	1.50	1.00	824.92	24.40	12.20	12.19	1.00
200x75-t1.5-B50	50	200.76	74.85	1.49	1.01	850.00	19.93	9.96	9.98	1.00
200x75-t1.5-B75	75	200.80	74.89	1.49	1.01	874.83	22.53	11.27	11.30	1.00
200x75-t1.5-B100	100	201.14	74.76	1.50	1.00	900.08	24.80	12.40	12.38	1.00
250x75-t1.5-B50	50	251.05	76.67	1.48	1.01	999.83	19.59	9.80	9.72	1.01
250x75-t1.5-B75	75	251.55	75.08	1.50	1.00	1025.00	22.02	11.01	11.02	1.00
250x75-t1.5-B100	100	252.19	75.09	1.49	1.01	1049.67	23.68	11.84	11.80	1.00
Flange restrained										
175x60-t1.5-B50	50	177.61	59.59	1.50	1.00	775.08	23.16	11.58	11.60	1.00
175x60-t1.5-B75	75	175.98	59.66	1.49	1.01	800.00	26.55	13.28	13.29	1.00
175x60-t1.5-B100	100	173.33	59.60	1.50	1.00	825.00	29.38	14.69	14.70	1.00
200x75-t1.5-B50	50	200.76	74.92	1.50	1.00	850.25	23.00	11.50	11.48	1.00
200x75-t1.5-B75	75	200.51	74.90	1.47	1.02	875.08	26.22	13.11	13.02	1.01
200x75-t1.5-B100	100	200.89	74.85	1.50	1.00	900.08	29.25	14.62	14.69	1.00
250x75-t1.5-B50	50	251.46	74.83	1.49	1.01	1000.00	22.81	11.41	11.40	1.00
250x75-t1.5-B75	75	251.62	74.74	1.48	1.01	1025.08	25.95	12.98	12.96	1.00
250x75-t1.5-B100	100	251.84	74.77	1.50	1.00	1050.00	28.98	14.49	14.41	1.01
Mean										1.00
COV										0.01

2.2 Sections coding

In Tables 1 and 2, the sections have been coded so that the nominal section dimension, and the length of the load and reaction plates can be determined from the coding system. As an example, the label “175×60-t1.5-B100-FU” can be explained as follows. The first and second annotations are the nominal sections depth and width in millimeters. The annotation "B100" indicates the load or reaction plate length in millimeters (i.e. 100 mm). ″FU″ indicates flange is unrestrained to the load and reaction plates while ″FR″ represents flange is restrained to the load and reaction plates. The same definitions were used in the numerical investigation.

2.3 Material properties

Tensile coupons were tested to determine the mechanical material properties of the sections. The coupons were prepared and tested in an Instron tensile testing machine according to ISO 6892-1 (2009). Ten coupons were taken from both the longitudinal and transverse directions of the ferritic stainless steel sheets from which the unlipped sections were press-braked. The average mechanical properties obtained from ten coupon tests (five tests for each direction) are presented in Table 3. Comparative hot-rolled steel stress strain curves can be found in Yousefi *et al.* (2014) and Rezvani *et al*. (2015).

Table 2 Measured section details and laboratory and finite element ultimate web crippling strengths under EOF load case for both flanges restrained and unrestrained to reaction plates

Section	Load bearing length	Web depth	Flange width	Web thickness	Filet ratio	Length of channel	Laboratory load full pair	Laboratory load per web	Finite element load per web	Comparison
	B *(mm)*	d *(mm)*	b_f *(mm)*	t *(mm)*	r_i/t *(mm)*	L *(mm)*	P_{LAB} *(kN)*	P_{LAB} *(kN)*	P_{FEA} *(kN)*	P_{LAB}/P_{FEA}
Flange unrestrained										
175x60-t1.5-B50	50	175.51	59.99	1.46	1.03	725.10	18.16	4.54	4.61	0.98
175x60-t1.5-B75	75	175.48	60.03	1.47	1.02	775.25	19.80	4.95	5.01	0.99
175x60-t1.5-B100	100	175.53	60.02	1.45	1.03	825.23	21.52	5.38	5.30	1.02
200x75-t1.5-B50	50	200.54	75.03	1.47	1.02	800.15	17.40	4.35	4.42	0.98
200x75-t1.5-B75	75	200.50	75.00	1.44	1.04	850.34	18.88	4.72	4.78	0.99
200x75-t1.5-B100	100	200.55	75.01	1.46	1.03	900.58	20.24	5.06	5.01	1.01
250x75-t1.5-B50	50	250.61	75.01	1.47	1.02	950.09	15.28	3.82	3.92	0.97
250x75-t1.5-B75	75	250.46	75.00	1.48	1.01	1000.15	16.12	4.03	4.12	0.98
250x75-t1.5-B100	100	250.58	74.99	1.45	1.03	1050.26	17.36	4.34	4.40	0.99
Flange restrained										
175x60-t1.5-B50	50	175.67	60.01	1.48	1.01	725.12	23.488	5.87	5.95	0.99
175x60-t1.5-B75	75	175.65	60.07	1.47	1.02	775.26	26.368	6.59	6.64	0.99
175x60-t1.5-B100	100	175.64	60.20	1.49	1.01	825.32	29.504	7.37	7.3	1.01
200x75-t1.5-B50	50	200.48	75.03	1.50	1.00	800.25	22.464	5.61	5.67	0.99
200x75-t1.5-B75	75	200.60	75.01	1.48	1.01	850.17	24.608	6.15	6.21	0.99
200x75-t1.5-B100	100	200.52	75.01	1.48	1.01	900.22	27.136	6.78	6.83	0.99
250x75-t1.5-B50	50	250.50	75.01	1.50	1.00	950.13	19.808	4.95	4.9	1.01
250x75-t1.5-B75	75	250.41	75.00	1.47	1.02	1000.64	21.312	5.32	5.42	0.98
250x75-t1.5-B100	100	250.53	74.99	1.49	1.01	1051.23	22.752	5.68	5.74	0.99
Mean										0.99
COV										0.01

Table 3 Mechanical properties obtained from tensile tests

Coupon section	Nominal thickness *(mm)*	Base metal thickness *(mm)*	Gauge width *(mm)*	Gauge length *(mm)*	Tensile yield strength ($\sigma_{0.2}$) *(MPa)*	Tensile ultimate strength (σ_u) *(MPa)*
Longitudinal direction	1.5	1. 47	20	141	280	454
Transverse direction	1.5	1.48	20	141	295	475
Average value	---	---	---	---	288	465

2.4 Laboratory test set-up

The sections were tested under IOF and EOF load cases as per guidelines from AISI S100 Specification (AISI 2016) and Young and Hancock (2001), as depicted in Figs 3 and 4. The channels were bolted through the webs to load transfer blocks to provide symmetrical loading. High strength steel of nominal 550 MPa yield strength were used for the load plates. The load plate was placed at the mid length of the channels, applying the transverse force through the flanges of the unlipped channels. Half rounds, at each end, simulating pin supports were used under the load transfer blocks in the line of applied transverse force. The Instron was used to apply a displacement load to the test sections with a load rate of 0.05 mm/min until failure. Figs. 5 to 8 present the web crippling test-setup under IOF and EOF loadings while Figs 6 and 8 show the test set-up for with the flanges of the channels restrained to the load and reaction plates, through bolting of the flanges to the load and reaction plates.

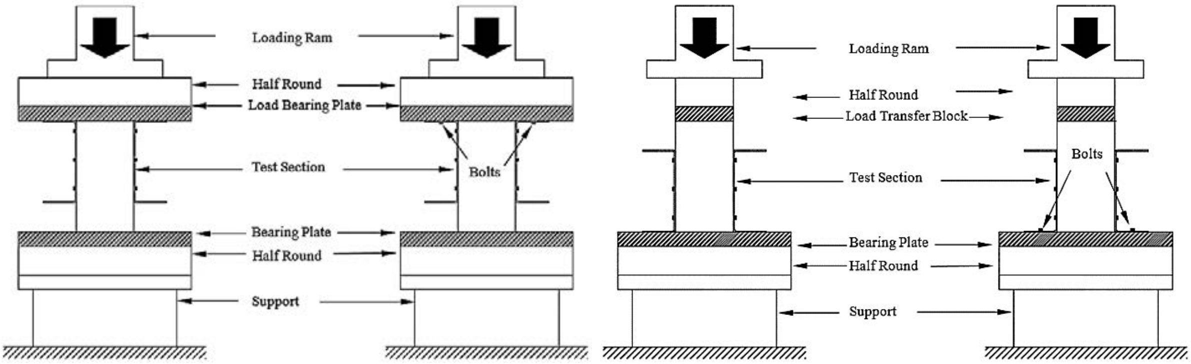

(a) IOF loading (b) EOF loading

Fig. 4 End view of test arrangement for both flanges restrained and unrestrained to load and reaction plates

2.5 Test results

In total, 36 unlipped channels were tested under IOF and EOF load cases. Tables 1 and 2 present the web crippling test ultimate load per single web, defined as P_{LAB}. Fig. 9 illustrates the typical web crippling failure mode of the sections for both flange loading conditions. Typical load-displacement responses from 200×75-t1.5-N75-FU and 200×75-t1.5-N75-FR, under the IOF and EOF load cases and for both flanges restrained and unrestrained to the load and reaction plates can be seen in Figs 10 and 11.

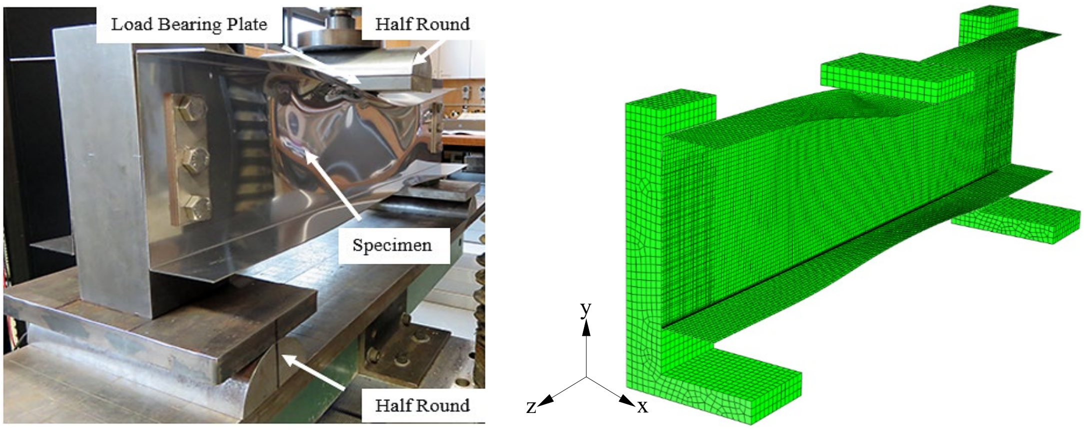

Fig. 5 Laboratory set-up and finite element analysis under IOF load case for unrestrained flanges

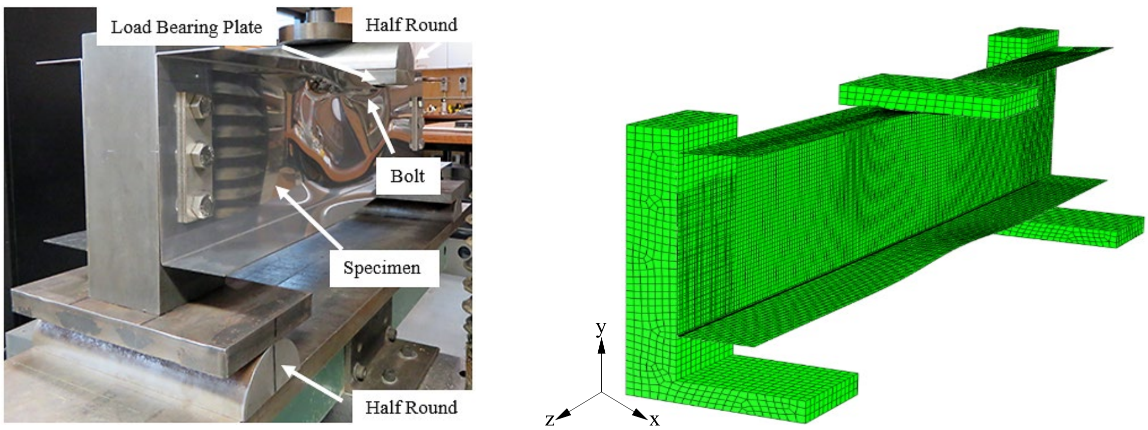

Fig. 6 Laboratory set-up and finite element analysis under IOF load case for restrained flanges

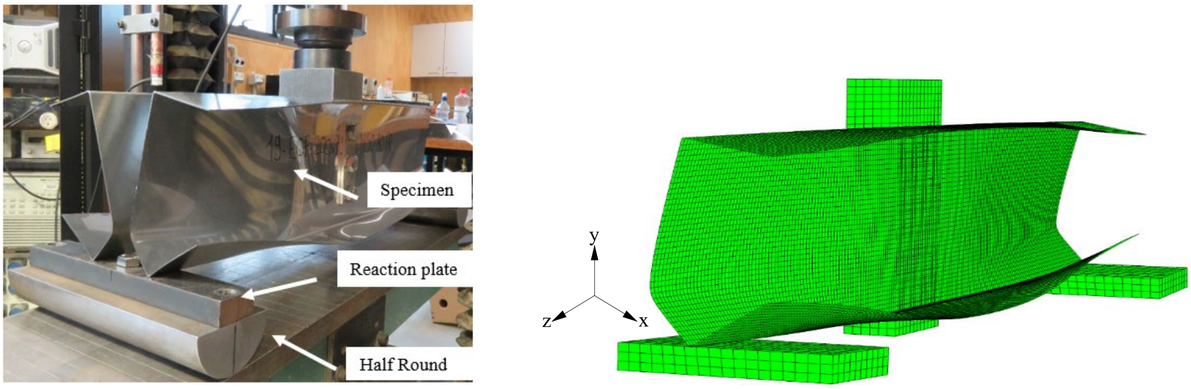

Fig. 7 Laboratory set-up and finite element analysis under EOF load case for unrestrained flanges

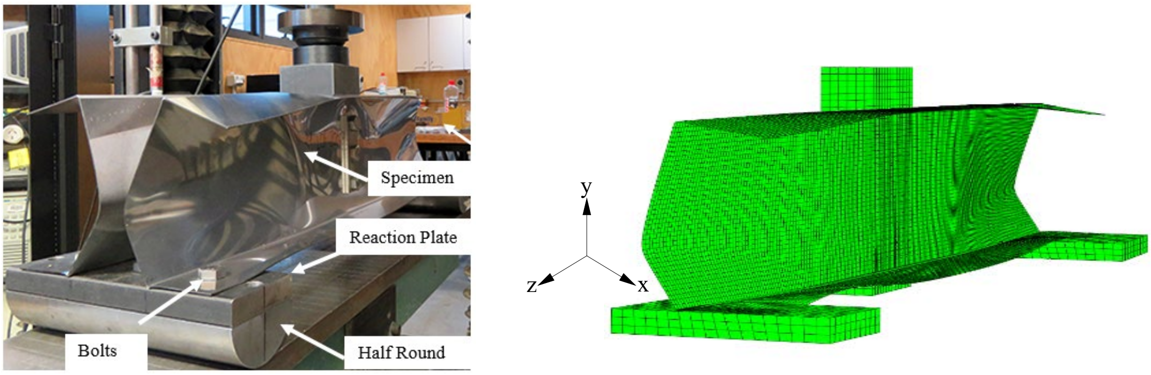

Fig. 8 Laboratory set-up and finite element analysis under EOF load case for restrained flanges

3 Numerical Investigation

In this paper, as mentioned in Section 1, the finite element analysis (FEA) models developed use quasi-static analyses with an implicit integration scheme in ABAQUS. In most previous studies in the literature, where the results of FEA or tests are subsequently used for reliability analysis and design rules proposed, such as those by Zhou and Young (2007c, 2013), Li and Young (2017a,b), Sundararajah et al. (2017), Nguyen et al. (2017), Sundararajah et al. (2016), Gunalan and Mahendran (2015), static analyses were used. However, as mentioned by Natario et al. (2014a,b), there is not always a good agreement in terms of post-buckling behaviour. For this reason, Natario et al. (2014a,b) proposed a quasi-static analyses with an explicit integration scheme.

However, as per the ABAQUS manual (2014), due to use of only a conditionally stable operator for integration of the equations of motion in explicit dynamic analysis, the size of the time increment in a such an analysis is limited; thus, it requires a large number of time increments for solving a problem which this leads to a longer computational time. Also, explicit analysis is more appropriate for very large problems, solving high speed discontinuous short-term events, and problems involving stress wave propagation. If explicit analysis is used for small scale problems with slow contact events, such as web crippling failure, complex and possibly unnecessary parameters would need to be needed to accelerate the solution and reduce the computational time, such as applying density and mass scaling factor, increasing load rate, modifying inertia effects.

In contrast, since having an unconditionally stable operator in implicit dynamic analysis, there is no limit on the size of the time increment which contributes to it being a more time efficient analysis and simpler to use for without considering unnecessary parameters. As per the ABAQUS manual, three important factors for approaching a nonlinear dynamic problem such as: the length of time for which the response is sought, the size of the problem; and the restrictions of the method.

As mentioned before, in this paper, the finite element analysis (FEA) models developed use quasi-static analyses with an implicit integration scheme in ABAQUS. Consistent with Natario et al. (2014a,b), for the quasi-static models with an implicit integration scheme, it was found that the post-buckling behaviour and elastic stiffness branches were closer to the laboratory results than static analysis. In addition, the quasi-static models with an implicit integration scheme has many advantages over the previous analyses types, such as improved convergence behaviour for determining essentially static solutions, applications with complex material nonlinearity and contacts. Also, quasi-static models with an implicit integration scheme can be used in a broad range of applications applicable for different numerical solution strategies with monotonic behaviour in which determining a final static response is interested.

3.1 Element type – material properties

The quadrilateral finite-membrane-strain S4R shell element was used for modelling the unlipped channels. S4R is a three-dimensional 4-node doubly curved thin element and is an appropriate element for most applications, especially for complex buckling behaviour for which it is known to provide accurate and robust solutions. The general purpose hexahedral C3D8R solid element, appropriate for three-dimensional modelling, was used for modelling the load plate. The unlipped channels were modelled using their measured centreline dimensions. The mean mechanical properties conducted from the tensile tests were also used for engineering stress-strain curve. As per the ABAQUS manual, the engineering material curve is converted into a true material curve:

$$\sigma_{true} = \sigma(1+\varepsilon) \quad (1)$$

$$\varepsilon_{true(pl)} = \ln(1+\varepsilon) - \frac{\sigma_{true}}{E} \quad (2)$$

3.2 Geometry and mesh

Figs. 5 to 8 show the laboratory test arrangement as modelled in the numerical study; as can be seen, symmetry was used. Typical finite element meshes, as well as the load bearing plates are shown. Finite element mesh sizes of 8 × 8 mm were used for the load bearing plate and 5 × 5 mm for the unlipped channels. Five elements were used for the corner region of the channels.

3.3 Boundary conditions and loading procedure

An analytical solid plate was used to simulate the load plate with a reference point constraining the top surface of the load plate. Symmetry was used for the surfaces of the load transfer blocks, thus also preventing rotation about the z and y axes and movement in the x direction. Vertical displacement was applied to the load plate through a reference point. The unlipped channels, load plate, and the interfaces between the unlipped channels and the load plate were modelled. ″Surface to surface″ contact was used for contact modelling between the load plate and flange. The flange was the slave surface, while the load plate was the master surface. Penetration was not allowed between the two contact surfaces. For simulating the bolts, Cartesian connectors were used.

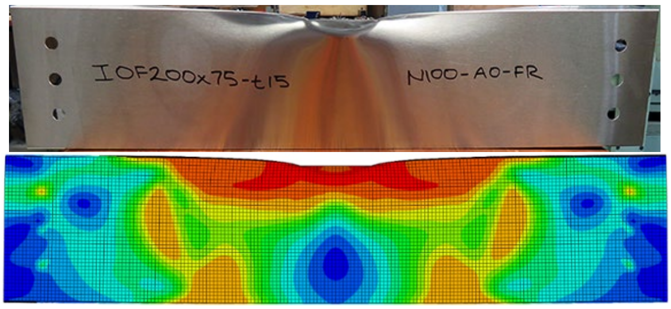

(a) Flanges unrestrained to load bearing plate

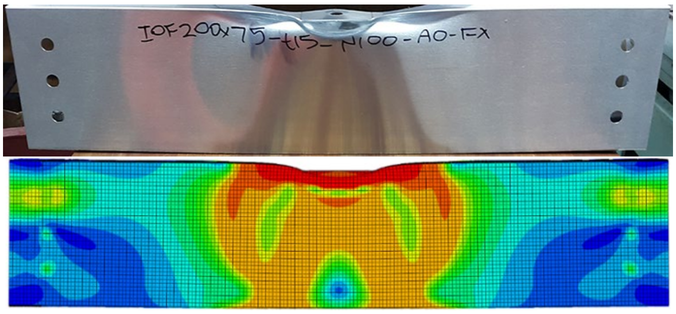

(b) Flanges restrained to load bearing plate

Fig. 9 Failure modes of the sections under IOF load case

3.4 *Finite element verification*

The laboratory and the finite element (FE) results were compared. The web crippling ultimate loads per single web (P_{LAB}) are presented in Tables 1 and 2. The mean ratio of the laboratory results over the FEA results are 1.00 and 0.99, with a coefficient of variation of COV=0.01. Overall, 3% was the maximum difference for the section 250x75-t1.5-B50-A0-FU obtained from the FEA and laboratory results for EOF load case. Figs. 10 and 11 compare the vertical load-displacement curves for section 200×75-t1.5 for unlipped channels under IOF and EOF load cases where flanges are restrained and unrestrained to the load and reaction plates. A good agreement is shown for both sections. As depicted in Fig. 9, the failure modes are compared against the FEA model. The failure modes from the finite element results were similar to the experimental failure modes.

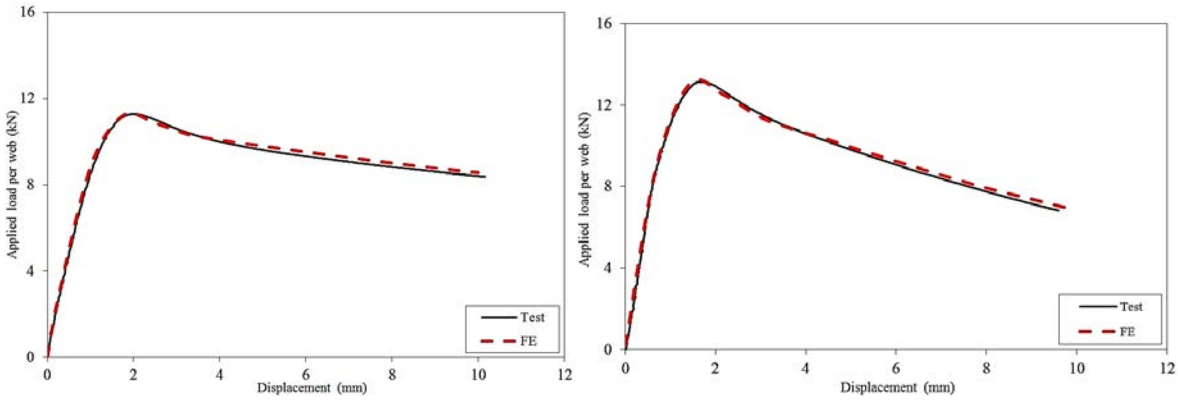

Fig. 10 Laboratory and numerical web deformation curves for section 200×75-t1.5-N75 under IOF load case; (a) Flanges unrestrained to load plate; (b) Flanges restrained to load plate

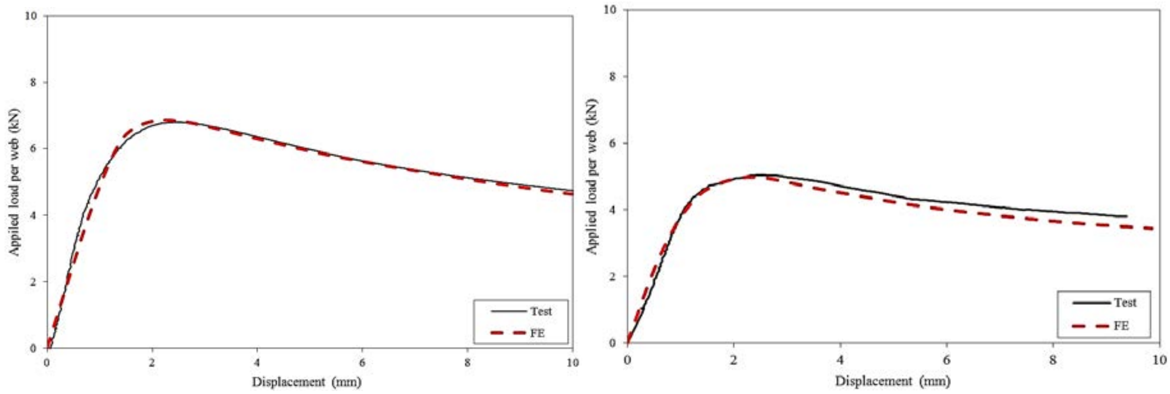

Fig. 11 Laboratory and numerical web deformation curves for section 200×75-t1.5-N100 under EOF load case; (a) Flanges restrained to load plate; (b) Flanges unrestrained to load plate

4 Parametric study

The FE model was used for a study on the web crippling strength of channels subjected to IOF and EOF load cases with flanges restrained and unrestrained to the load and reaction plates. The parameters considered included different lengths of the load and reaction plates. The cross-section sizes and thicknesses of the unlipped channels were also varied to obtain web crippling strengths for different load and reaction plates lengths ratios *(B/h and B/t)* and height to thickness ratios (*h/t*). The unlipped channels had different depth sizes, with thicknesses (*t*) between 1.45 mm to 6.0 mm. The height-to thickness ratios (*h/t*) were between 148.92 to 232.63. The length of load and reaction plates (*B*) were 50 mm, 75 mm and 100 mm. The load and reaction plates, applying the concentrated forces, were thus considered to cover the full flange widths of the unlipped channels.

The models have been coded so that the nominal model dimension and the length of the load or reaction plates can be identified. The web crippling strengths per single web predicted from the FEA as well as laboratory results for different cross-section dimensions were determined. it is found out that the ultimate web crippling strengths are affected by the length of the load and reaction plates as well as section thicknesses. As expected, the web crippling strengths increase with the length of the load and reaction plates. It also can be seen that the results obtained from the unlipped channels with flanges restrained to the load and reaction plates are on average 16% higher than those of the unrestrained unlipped channels.

5 Design comparisons for cold-formed ferritic stainless steel channels

As noted previously, no cold-formed stainless steel standard distinguishes between flanges restrained and unrestrained to the load and reaction plates i.e. each standard only provides one equation for both flange conditions. However, as seen in laboratory and numerical studies, the web crippling strengths vary considerably with regards to the flange condition. The web crippling strengths obtained from the laboratory and numerical studies are compared to strengths predicted from the stainless steel standards in order to evaluate the accuracy and suitability of current standards.

In Tables 3 to 4, the web crippling strengths obtained from laboratory and numerical studies are compared with the results predicted from design standards for the unlipped channels. Table 6 presents the design comparisons for the IOF load case with flange unrestrained to the load bearing plate. In the EN 1993-1-4 (CEN 2006) comparison, the mean ratio of the laboratory and numerical results over the results predicted from EN 1993-1-4 standard is 1.10, giving a coefficient of variation of COV=0.06. From the Australian standard (AS/NZS 4673), as well as the American specification (SEI/ASCE-8) comparisons, the mean ratios are 0.99 and 1.00, respectively, with coefficients of variation of COV=0.06. Current stainless steel standards are thus shown to predict the web crippling strength with a 10% conservatism for the IOF load case with flange unrestrained to the load bearing plate.

Table 3 shows the design comparisons for the EOF load case with flange unrestrained to the reaction plates. In the EN 1993-1-4 (CEN 2006) comparison, the mean ratio of the laboratory and numerical results over the results predicted from the EN 1993-1-4 standard is 1.37, giving a coefficient of variation of COV=0.15. From the Australian standard (AS/NZS 4673) as well as the American specification (SEI/ASCE-8) comparisons, the mean ratios are 1.23 and 1.24, with the same coefficient of variation of COV=0.15. Current stainless steel standards are thus shown to predict the web crippling strength with a 37% conservatism for the EOF load case with flanges unrestrained to the reaction plates.

Table 4 shows the same design comparisons for the EOF load case with flange restrained to the reaction plates. In the EN 1993-1-4 (CEN 2006) comparison, the mean ratio of the laboratory and numerical results over the results predicted from the EN 1993-1-4 standard is 1.58, giving a coefficient of variation of COV=0.13. From the Australian standard (AS/NZS 4673) as well as the American specification (SEI/ASCE-8) comparisons, the mean ratios are 1.43 and 1.48, with the same coefficient of variation of COV=0.12. Current stainless steel standards are thus shown to predict the web crippling strength with a 58% conservatism for the EOF load case with flanges restrained to the reaction plates.

It therefore be seen that EN 1993-1-4 have a more conservative approach towards predicting the web crippling strengths, in comparison to the Australian standard (AS/NZS 4673) and American specification (SEI/ASCE-8). A comparison of the obtained values from the aforementioned standards with the results from the laboratory and numerical studies shows that the strength predictions from the SEI/ASCE-8 specification are 48% higher when compared to the laboratory and numerical failure loads for the EOF load case. The current web crippling designs are therefore conservative to employ for cold-formed ferritic stainless steel unlipped channels, under IOF and EOF load cases with flanges restrained and unrestrained to the load and reaction plates.

Table 3 Comparison of laboratory and numerical web crippling strengths with design regulations under EOF load case for flanges unrestrained to reaction plates

Section	Failure load	Web crippling strength per web predicted from current design standards				Comparison			
	P_F (kN)	P_{ASCE} (kN)	$P_{AS/NZS}$ (kN)	P_{Euro} (kN)	P_{NAS} (kN)	P_F/P_{ASCE}	$P_F/P_{AS/NZS}$	P_F/P_{Euro}	P_F/P_{NAS}
EOF 175×60-t1.5-B50- FU	4.54	3.90	3.89	3.53	4.11	1.16	1.17	1.29	1.10
EOF 175×60-t4.0-B50- FU	40.29	29.43	29.61	26.49	35.01	1.37	1.36	1.52	1.15
EOF 175×60-t6.0-B50- FU	74.92	65.03	65.48	58.52	76.45	1.15	1.14	1.28	0.98
EOF 175×60-t1.5-B75- FU	4.95	4.60	4.59	4.15	5.06	1.08	1.08	1.19	0.98
EOF 175×60-t4.0-B75- FU	44.26	31.06	31.26	27.96	40.35	1.42	1.42	1.58	1.10
EOF 175×60-t6.0-B75- FU	73.24	67.54	67.99	60.78	87.34	1.08	1.08	1.21	0.84
EOF 175×60-t1.5-B100- FU	5.38	4.93	4.91	4.62	5.44	1.09	1.10	1.16	0.99
EOF 175×60-t4.0-B100-FU	44.16	32.70	32.90	29.43	44.86	1.35	1.34	1.50	0.98
EOF 175×60-t6.0-B100- FU	71.29	70.04	70.51	63.03	96.52	1.02	1.01	1.13	0.74
EOF 200×75-t1.5-B50- FU	4.35	3.96	3.96	3.58	4.16	1.10	1.10	1.22	1.05
EOF 200×75-t4.0-B50- FU	40.73	29.18	29.35	26.26	34.40	1.40	1.39	1.55	1.18
EOF 200×75-t6.0-B50-FU	85.81	64.67	65.10	58.20	75.40	1.33	1.32	1.47	1.14
EOF 200×75-t1.5-B75- FU	4.72	4.47	4.47	4.04	4.89	1.05	1.06	1.17	0.97
EOF 200×75-t4.0-B75- FU	45.81	30.80	30.98	27.72	39.65	1.49	1.48	1.65	1.16
EOF 200×75-t6.0-B75- FU	86.45	67.16	67.60	60.44	86.14	1.29	1.28	1.43	1.00
EOF 200×75-t1.5-B100- FU	5.06	4.86	4.84	4.55	5.33	1.04	1.05	1.11	0.95
EOF 200×75-t4.0-B100- FU	53.63	32.42	32.61	29.18	44.08	1.65	1.64	1.84	1.22
EOF 200×75-t6.0-B100- FU	84.30	69.65	70.11	62.68	95.20	1.21	1.20	1.35	0.89
EOF 250×100-t1.5-B50- FU	3.82	3.69	3.68	3.34	3.83	1.03	1.04	1.14	1.00
EOF 250×100-t4.0-B50- FU	37.74	28.67	28.83	25.81	33.29	1.32	1.31	1.46	1.13
EOF 250×100-t6.0-B50- FU	86.07	63.95	64.35	57.55	73.49	1.35	1.34	1.50	1.17
EOF 250×100-t1.5-B75- FU	4.03	4.17	4.15	3.77	4.50	0.97	0.97	1.07	0.90
EOF 250×100-t4.0-B75- FU	41.41	30.27	30.44	27.25	38.38	1.37	1.36	1.52	1.08
EOF 250×100-t6.0-B75- FU	92.99	66.41	66.83	59.77	83.97	1.40	1.39	1.56	1.11
EOF 250×100-t1.5-B100- FU	4.34	4.65	4.63	4.35	5.06	0.93	0.94	1.00	0.86
EOF 250×100-t4.0-B100- FU	45.60	31.86	32.04	28.68	42.66	1.43	1.42	1.59	1.07
EOF 250×100-t6.0-B100- FU	95.04	68.86	69.30	61.98	92.80	1.38	1.37	1.53	1.02
Mean value, (P_m)						1.24	1.23	1.37	1.03
Coefficient of variation, (V_p)						0.15	0.15	0.15	0.12

Table 4 Comparison of laboratory and numerical web crippling strengths with design regulations under EOF load case for flanges restrained to reaction plates

Section	Failure load	Web crippling strength per web predicted from current design standards				Comparison			
	P_F (kN)	P_{ASCE} (kN)	$P_{AS/NZS}$ (kN)	P_{Euro} (kN)	P_{NAS} (kN)	P_F/P_{ASCE}	$P_F/P_{AS/NZS}$	P_F/P_{Euro}	P_F/P_{NAS}
EOF 175×60-t1.5-B50- FR	5.872	3.88	4.01	3.63	4.83	1.51	1.47	1.62	1.22
EOF 175×60-t4.0-B50- FR	45.016	28.46	29.61	26.49	32.82	1.58	1.52	1.70	1.37
EOF 175×60-t6.0-B50- FR	77.024	62.89	65.47	58.52	69.44	1.22	1.18	1.32	1.11
EOF 175×60-t1.5-B75- FR	6.592	4.39	4.53	4.10	5.56	1.50	1.46	1.61	1.18
EOF 175×60-t4.0-B75- FR	46.968	30.04	31.26	27.96	36.90	1.56	1.50	1.68	1.27
EOF 175×60-t6.0-B75- FR	76.312	65.31	67.99	60.77	77.28	1.17	1.12	1.26	0.99
EOF 175×60-t1.5-B100- FR	7.376	4.83	4.98	4.67	6.10	1.53	1.48	1.58	1.21
EOF 175×60-t4.0-B100-FR	45.832	31.62	32.90	29.43	40.34	1.45	1.39	1.56	1.14
EOF 175×60-t6.0-B100- FR	74.904	67.73	70.51	63.02	83.89	1.11	1.06	1.19	0.89
EOF 200×75-t1.5-B50- FR	5.616	3.73	3.84	3.48	4.68	1.51	1.46	1.61	1.20
EOF 200×75-t4.0-B50- FR	44.288	28.22	29.35	26.26	32.47	1.57	1.51	1.69	1.36
EOF 200×75-t6.0-B50-FR	87.872	62.55	65.10	58.20	68.85	1.40	1.35	1.51	1.28
EOF 200×75-t1.5-B75- FR	6.152	4.15	4.28	3.88	5.31	1.48	1.44	1.58	1.16
EOF 200×75-t4.0-B75- FR	53.904	29.79	30.98	27.72	36.51	1.81	1.74	1.94	1.48
EOF 200×75-t6.0-B75- FR	88.656	64.95	67.60	60.44	76.62	1.36	1.31	1.47	1.16
EOF 200×75-t1.5-B100- FR	6.784	4.70	4.84	4.55	5.98	1.44	1.40	1.49	1.13
EOF 200×75-t4.0-B100- FR	54.016	31.35	32.61	29.18	39.91	1.72	1.66	1.85	1.35
EOF 200×75-t6.0-B100- FR	87.32	67.36	70.11	62.68	83.18	1.30	1.25	1.39	1.05
EOF 250×100-t1.5-B50- FR	4.952	3.52	3.62	3.29	4.50	1.41	1.37	1.50	1.10
EOF 250×100-t4.0-B50- FR	42.928	27.73	28.83	25.81	31.83	1.55	1.49	1.66	1.35
EOF 250×100-t6.0-B50- FR	89.168	61.84	64.35	57.55	67.76	1.44	1.39	1.55	1.32
EOF 250×100-t1.5-B75- FR	5.328	3.92	4.03	3.67	5.12	1.36	1.32	1.45	1.04
EOF 250×100-t4.0-B75- FR	52.344	29.28	30.44	27.25	35.79	1.79	1.72	1.92	1.46
EOF 250×100-t6.0-B75- FR	97.416	64.22	66.83	59.77	75.42	1.52	1.46	1.63	1.29
EOF 250×100-t1.5-B100- FR	5.688	4.44	4.56	4.30	5.76	1.28	1.25	1.32	0.99
EOF 250×100-t4.0-B100- FR	58.016	30.81	32.04	28.68	39.13	1.88	1.81	2.02	1.48
EOF 250×100-t6.0-B100- FR	96.568	66.60	69.30	61.98	81.87	1.45	1.39	1.56	1.18
Mean value, (P_m)						1.48	1.43	1.58	1.21
Coefficient of variation, (V_p)						0.12	0.12	0.13	0.13

6 Proposed design equations and comparison with experimental and numerical analyses results

As noted previously, stainless steel design specifications, particularly EN 1993-1-4 (CEN 2006) as well as SEI/ASCE-8 (ASCE 2002) provide conservative web crippling strength predictions for cold-formed ferritic stainless steel unlipped channels. Thus, based on the laboratory and numerical results from this study, web crippling equations for such channels with flanges restrained and unrestrained to the load and reaction plates under the IOF and EOF load cases are proposed. The following proposed web crippling equations apply similar equations as to AISI S100 Standard (AISI 2016):

IOF load case:

Flange is unrestrained to load bearing plate:

$$P_p = 10.5 t^2 f_y \sin\theta \left(1 - 0.28\sqrt{\frac{R}{t}}\right)\left(1 + 0.23\sqrt{\frac{N}{t}}\right)\left(1 - 0.01\sqrt{\frac{h}{t}}\right) \quad (5)$$

Flange is restrained to load bearing plate:

$$P_p = 14.3t^2 f_y \sin\theta \left(1 - 0.23\sqrt{\frac{R}{t}}\right)\left(1 + 0.15\sqrt{\frac{N}{t}}\right)\left(1 - 0.01\sqrt{\frac{h}{t}}\right) \quad (6)$$

EOF load case:

Flanges are unrestrained to reaction plates:

$$P_p = 7t^2 f_y \sin\theta \left(1 - 0.10\sqrt{\frac{R}{t}}\right)\left(1 + 0.23\sqrt{\frac{N}{t}}\right)\left(1 - 0.04\sqrt{\frac{h}{t}}\right) \quad (7)$$

Flanges are restrained to reaction plates:

$$P_p = 6.3t^2 f_y \sin\theta \left(1 - 0.20\sqrt{\frac{R}{t}}\right)\left(1 + 0.24\sqrt{\frac{N}{t}}\right)\left(1 - 0.02\sqrt{\frac{h}{t}}\right) \quad (8)$$

In these equations, "h" is the plain part of the web depth, "t" defines as the web thickness, "f_y" indicates $\sigma_{0.2}$ of proof stress (yield stress), "θ" defines the angle between the bearing surface and the channel web, and "N" is the load and reaction plates lengths. The limitations for the web crippling equations (7) are $N/t \leq 70.92$, $h/t \leq 175$, and $N/h \leq 0.61$.

7 Comparison of the proposed design equations with laboratory and numerical analyses results

As shown in Tables 5 and 6, the ultimate web crippling strengths per single web (P_{LAB} and P_{FEA}) from laboratory and numerical studies are compared with the predicted values from the proposed design strengths (P_P) using equations (5-8). As can be seen from Tables 5 and 6, the proposed equations for cold-formed ferritic stainless steel unlipped channels generally provide conservative and reliable web crippling strength predictions.

In terms of flanges restrained to the load and reaction plates, it is evident from Table 5 that the mean of the obtained web crippling strength values from the numerical and the laboratory analyses results over the results from the proposed equations is 1.00, having coefficient of variations of COV=0.06 and 0.08 and having corresponding reliability index values of β=2.56 and 2.51, for IOF and EOF load cases, respectively. In regard to flanges unrestrained to the load and reaction plates, it is clear from Table 6 that the mean ratio of the obtained web crippling strength values from the laboratory and numerical results over the results from the proposed web crippling equation is also 1.00, having coefficient of variations of COV=0.04 and 0.07 and having corresponding reliability index values of β=2.61 and 2.53, for IOF and EOF load cases, respectively. Thus, the equations proposed for ferritic stainless steel unlipped channels with restrained and unrestrained flanges reliability predict the web crippling strength of such channels under the IOF and EOF load cases.

Table 5 Web crippling strength comparison for IOF and EOF load cases for restrained flanges

IOF and EOF	ASCE		AS/NZs		EC3		NAS		Proposed	
	P_F/P_{ASCE}		$P_F/P_{AS/NZs}$		P_F/P_{EC3}		P_F/P_{NAS}		$P_F/P_{proposed}$	
	IOF	EOF	IOF	EOF	IOF	EOF	IOF	EOF	IOF	EOF
Mean (P_m)	1.16	1.48	1.15	1.43	1.28	1.58	1.12	1.21	1.00	1.00
COV (V_p)	0.08	0.12	0.08	0.12	0.08	0.13	0.06	0.13	0.06	0.08
Resistance factor (ϕ)									0.85	0.85
Reliability index (β)									2.56	2.51

Table 6 Web crippling strength comparison for IOF and EOF load cases for unrestrained flanges

IOF and EOF	ASCE		AS/NZs		EC3		NAS		Proposed	
	P_F/P_{ASCE}		$P_F/P_{AS/NZs}$		P_F/P_{EC3}		P_F/P_{NAS}		$P_F/P_{proposed}$	
	IOF	EOF	IOF	EOF	IOF	EOF	IOF	EOF	IOF	EOF
Mean (P_m)	1.00	1.24	0.99	1.23	1.10	1.37	1.19	1.03	1.00	1.00
COV (V_p)	0.06	0.15	0.06	0.15	0.06	0.15	0.09	0.12	0.06	0.08
Resistance factor (ϕ)									0.85	0.85
Reliability index (β)									2.56	2.51

8 Conclusions

The web crippling strength of cold-formed ferritic stainless steel unlipped channels subject to interior-one-flange (IOF) and end-one-flange (EOF) loading have been considered in this paper. A total of 144 results have been presented, comprising 36 laboratory and 108 numerical results; the cases of flanges restrained and unrestrained to the load and reaction plates were covered. In most previous studies mentioned in the introduction, static analyses were used. However, as mentioned by Natario et al. (2014a,b), there is not always a good agreement in terms of post-buckling behaviour. For this reason, Natario et al. (2014a,b) proposed a quasi-static analyses with an explicit integration scheme. However, as per the ABAQUS manual (2014), due to use of only a conditionally stable operator for integration of the equations of motion in explicit dynamic analysis, the size of the time increment in a such an analysis is limited; thus, it requires a large number of time increments for solving a problem which this leads to a longer computational time. Also, explicit analysis is more appropriate for very large problems, solving high speed discontinuous short-term events, and problems involving stress wave propagation. Thus, unlike other works in the literature, the numerical analysis in this paper uses a nonlinear quasi-static finite element analysis with an implicit integration scheme.

The laboratory and numerical investigations have shown current stainless steel design guidance to be conservative. In terms of design standards, while no cold-formed stainless steel standard distinguishes between flanges restrained and unrestrained to the load and reaction plates, with each standard providing only one equation to cover both restrained and unrestrained conditions, the web crippling strengths for the flanges unrestrained case were found to be higher than those predicted from SEI/ASCE-8 by as much as 24%. Also, the web crippling strengths for the flanges restrained case were shown to be higher than those predicted from equations found in the literature by as much as 48%. New web crippling design equations have been proposed; the proposed equations have been shown to be reliable when compared against the laboratory and numerical results.

References

ABAQUS version 6.14-2 [Computer software]. Dassault Systemes, Waltham, MA, 2014.

American Iron and Steel Institute Specification (AISI). (2016). "North American Specification for the Design of Cold-Formed Steel Structural Members."AISI S100-16, Washington, D.C.

American Society of Civil Engineers (ASCE). (2010). "Minimum design loads for buildings and other structures." SEI/ASCE 7-10, New York.

American Society of Civil Engineers (ASCE). (2002). "Specification for the design of cold-formed stainless steel structural members." SEI/ASCE 8-02, Reston,Va.

Australian/New Zealand Standard (AS/NZS). (2001). "Cold-formed stainless steel structures." *AS/NZS 4673:2001*, Standards Australia, Sydney, Australia.

Cashell, K. A., and Baddoo, N. R. (2014). "Ferritic stainless steels in structural applications." *Thin-Wall. Struct.*, 83, 169-181.

CEN (European Committee for Standardization. (2006). "Design of steel structures: Part 1.4: General rules: Supplementary rules for stainless steels." *Eurocode 3, EN 1993-1-4,* Brussel, Belgium.

CEN (European Committee for Standardization. (2006). "General rules: Supplementary rules for cold-formed members and sheeting." *Eurocode 3, EN 1993-1-3,* Brussel, Belgium.

Gunalan, S., and Mahendran, M. (2015). "Web crippling tests of cold-formed steel channels under two flange load cases." J. Constr. Steel Res., 110, 1-15.

ISO E. 6892-1. (2009). "Metallic Materials: Tensile Testing: Part 1: Method of Test at Room Temperature" *ISO E. 6892-1*, International Standard, Geneva.

Korvink, S. A., Van den Berg, G. J., and Van der Merwe, P. (1995). "Web crippling of stainless steel cold-formed beams." *J. Constr. Steel Res.*, 34(2-3), 225-248.

Korvink, S. A., Van den Berg, G. J. (1994). "Web crippling of stainless steel cold-formed beams." *Proc., 12th Int. Specialty Conf. on Cold-Formed Steel Structures, University of Missouri-Rolla, St. Louis, 551-569.*

Lawson, R. M., Basta, A., and Uzzaman, A. (2015). "Design of stainless steel sections with circular openings in shear." *J. Constr. Steel Res.*, 112, 228-241.

Lian, Y., Uzzaman, A., Lim, J. B. P., Abdelal, G., Nash, D., and Young, B. (2017). "Web crippling behaviour of cold-formed steel channel sections with web holes subjected to Interior-one-flange loading condition-part I: experimental and numerical investigation." *Thin-Wall. Struct.*, 111, 103-112.

Lian, Y., Uzzaman, A., Lim, J. B. P., Abdelal, G., Nash, D., and Young, B. (2016). "Effect of web holes on web crippling strength of cold-formed steel channel sections under end-one-flange loading condition– Part I: Tests and finite element analysis." *Thin-Wall. Struct.*, 107, 443-452.

Li, H. T., and Young, B. (2017a). "Cold-formed ferritic stainless steel tubular structural members subjected to concentrated bearing loads." *Eng. Struct.*, 145, 392-405.

Li, H. T., and Young, B. (2017b). "Tests of cold-formed high strength steel tubular sections undergoing web crippling." *Eng. Struct.*, 141, 571-583.

Mohammadjani, C., Yousefi, A. M., Cai, S. Q., Clifton, G. C., and Lim, J. B. P. (2017). "Strength and stiffness of cold-formed steel portal frame joints using quasi-static finite element analysis." *Steel Compos. Struct.*, Int. J., *25*(6), 727-734.

Natario, P., Silvestre, N., and Camotim, D. (2014a). "Web crippling failure using quasi-static FE models." *Thin-Wall. Struct.*, *84*, 34-49.

Natario, P., Silvestre, N., and Camotim, D. (2014b). "Computational modelling of flange crushing in cold-formed steel sections." *Thin-Wall. Struct.*, *84*, 393-405.

Rezvani, F. H., Yousefi, A. M., Ronagh, H. R. (2015). "Effect of span length on progressive collapse behaviour of steel moment resisting frames". *Structures,* 3, 81-89.

Uzzaman, A., Lim, J. B. P., Nash, D., Rhodes, J., and Young, B. (2012). "Web crippling behaviour of cold-formed steel channel sections with offset web holes subjected to interior-two-flange loading." *Thin-Wall. Struct.*, 50, 76-86.

Uzzaman, A., Lim, J. B. P., Nash, D., Rhodes, J., and Young, B. (2013). "Effect of offset web holes on web crippling strength of cold-formed steel channel sections under end-two-flange loading condition." *Thin-Wall. Struct.*, 65, 34-48.

Young, B., and Hancock, G. J. (2001). "Design of cold-formed channels subjected to web crippling." *J. Struct. Eng.*, 10.1061/(ASCE)0733-9445(2001)127:10(1137), 1137-1144.

Yousefi, A. M., Lim, J. B. P., and Clifton, G. C. (2018). Web crippling behaviour of unlipped cold-formed ferritic stainless steel channels subject to one-flange loading, *J. Struct. Eng.*, DOI: 10.1061/(ASCE)ST.1943-541X.0002118.

Yousefi, A. M., Lim, J. B. P., Uzzaman, A., Lian, Y., Clifton, G. C., and Young, B. (2017a). "Design of cold-formed stainless steel lipped channel sections with web openings subjected to web crippling under end-one-flange loading condition." *Adv. Struct. Eng.*, 20(7), 1024-1045.

Yousefi, A. M., Uzzaman, A., Lim, J. B. P., Clifton, G. C., and Young, B. (2017b). "Numerical investigation of web crippling strength in cold-formed stainless steel lipped channels with web openings subjected to interior-two-flange loading condition." *Steel Compos. Struct.*, Int. J., *23*(4), 363-383.

Yousefi, A. M., Uzzaman, A., Lim, J. B. P., Clifton, G. C., and Young, B. (2017c). "Web crippling strength of cold-formed stainless-steel lipped channels with web perforations under end-two-flange loading." *Adv. Struct. Eng.*, 20(12), 1845-1863.

Yousefi, A. M., Lim, J. B. P., and Clifton, G. C. (2017d). "Cold-formed ferritic stainless steel unlipped channels with web openings subjected to web crippling under interior-two-flange loading condition-part I: Tests and finite element model validation." *Thin-Wall. Struct.,* 116, 333-341.

Yousefi, A. M., Lim, J. B. P., and Clifton, G. C. (2017e). "Cold-formed ferritic stainless steel unlipped channels with web openings subjected to web crippling under interior-two-flange loading condition-part II: Parametric Study and design equations." *Thin-Wall. Struct.,* 116, 342-356.

Yousefi, A. M., Lim, J. B. P., and Clifton, G. C. (2017f). "Web bearing capacity of ulipped cold-formed ferritic stainless steel channels with perforated web subject to end-two-flange (ETF) loading." *Eng. Struct*., 152, 804-818.

Yousefi, A. M., Lim, J. B. P., Uzzaman, A., Lian, Y., Clifton, G. C., and Young, B. (2016a). "Web crippling strength of cold-formed stainless steel lipped channel-sections with web openings subjected to interior-one-flange loading condition." *Steel Compos. Struct.*, Int. J., *21*(3), 629-659.

Yousefi, A. M., Lim, J. B. P., Uzzaman, A., Lian, Y., Clifton, G. C., and Young, B. (2016b). " Web Crippling Strength of Cold-Formed Duplex Stainless Steel Lipped Channel-Sections with Web Openings Subjected to Interior-One-Flange Loading Condition."*Proc., Wei-Wen Yu Int. Specialty Conf. on Cold-Formed Steel Structures,* Univ. of Missouri-Rolla, Missouri, 313-324.

Yousefi, A. M., Hosseini M., Fanaie, N. (2014). "Vulnerability Assessment of Progressive Collapse of Steel Moment Resistant Frames." *Trends in Applied Sciences Research, 9 450-460.*

Zhou, F., and Young, B. (2013). "Web crippling behaviour of cold-formed duplex stainless steel tubular sections at elevated temperatures." *Eng. Struct.*, 57, 51-62.

Zhou, F., and Young, B. (2010). "Web crippling of aluminium tubes with perforated webs." *Eng. Struct.*, 32(5), 1397-1410.

Zhou, F., Young, B., and Zhao, X. L. (2009). "Tests and design of aluminum tubular sections subjected to concentrated bearing load." *J. Struct. Eng.*, 10.1061/(ASCE)ST.1943-541X.0000015, 806-817.

Zhou, F., and Young, B. (2007a). "Cold-formed high-strength stainless steel tubular sections subjected to web crippling." *J. Struct. Eng.,* 10.1061/(ASCE)0733-9445(2007)133:3(368), 368-377.

Zhou, F., and Young, B. (2007b). "Experimental and numerical investigations of cold-formed stainless steel tubular sections subjected to concentrated bearing load." J. Constr. Steel Res., 63(11), 1452-1466.

Zhou, F., and Young, B. (2006). "Cold-formed stainless steel sections subjected to web crippling." J. Struct. Eng., 10.1061/(ASCE)0733-9445(2006)132:1(134), 134-144